

DROPLET SIZE DISTRIBUTION AND LIQUID VOLUME CONCENTRATION  
IN A WATER SPRAY: PREDICTIONS AND MEASUREMENTS

Gabriel P. Pita  
Instituto Superior Técnico  
Dep. Engenharia Mecânica  
1096 Lisbon  
Portugal

**AD-P003 141**

**SUMMARY**

A water spray, from a twin-fluid atomizer, was studied at different air temperature and at atmospheric pressure.

The Sauter Mean Diameter,  $D_{32}$ , and the droplet volume distribution were measured at four different distances from the injector.

An optical method was used to measure droplet sizes.

Predictions of the Sauter Mean Diameter, liquid volume concentration and droplet size distribution were also evaluated. The influence of the air velocity, air temperature and of the water flow rate in the spray S.M.D. and in the liquid volume concentration at different distances from the injector have been measured. The predictions showed good agreement with experimental results.

**NOMENCLATURE**

- A - Droplet surface area
- $C_p$  - Specific heat of droplet liquid
- $C_v$  - Liquid volume concentration
- $D_{32}$  - Spray Sauter Mean Diameter (S.M.D.)
- h - Heat transfer coefficient
- $h_{fg}$  - Latent heat of vaporization
- M - Droplet mass
- $P_r$  - Prandtl number
- R - Droplet radius
- $R_e$  - Droplet Reynolds number,  $Re = \frac{\rho u_{rel} D_d}{\mu}$
- $T_\infty$  - Air temperature
- $T_d$  - Droplet temperature
- $u_{rel}$  - Relative velocity of the droplet to the mean stream
- $\rho, \mu$  - Gas properties evaluated at a film temperature =  $\left( \frac{T_\infty + T_d}{2} \right)$
- $\rho_l$  - Liquid density

**1. INTRODUCTION**

Knowing the behavior of an evaporating liquid droplet is essential to the understanding and prediction of the performance of the spray.

The behavior of the liquid fuel spray plays an important role in the combustion efficiency and in the production of the pollutants in combustion chambers.

Theoretical studies of evaporating sprays have been carried out by several authors [1,2,3,4,5,9], however their validation with experimental data has not often been attempted, mainly due to the difficulty in getting experimental results.

The present work includes a theoretical analysis of the evolution of a water spray, given an initial measured droplet distribution, characterised by a modified Rink distribution function [8], and a comparison of the predicted values with the measured ones at three different downstream locations along the spray axis. The droplet distribution has been divided into a discrete number of size groups with single droplet equations applied to each one of them. The droplet size measurements were made using an optical technique, based on the diffraction pattern formed when the droplets are illuminated by a parallel beam of monochromatic, coherent light [7,9,11].

**2. THEORY**

The assumptions used were the following

- 1: Droplet with spherical symmetry

- 2: Large distance between droplets
- 3: Physical properties varying with temperature
- 4: Constant pressure
- 5: Uniform droplet temperature
- 6: No radiation heat transfer

### 2.1 Droplet heat balance

The heat balance of a droplet exposed to a hot environment is expressed by the equation:

$$h A (T_{\infty} - T_d) = M \cdot C_p \cdot \frac{dT_d}{dt} + h_{fg} \frac{dM}{dt} \quad (1)$$

The convected heat is equal to the increase of internal energy plus the latent heat of vaporization.

In the first period of the droplet life the vaporization rate  $dM/dt$  is small compared with the increase in internal energy, so it can be assumed that the convected heat is equal to the increase in internal energy of the droplet. When the droplet temperature reaches the equilibrium vaporization temperature, the temperature remains constant ( $dT_d/dt = 0$ ) and the rate of heat transmission determine the vaporization rate of the droplet. As the air temperature is much greater than the droplet boiling temperature, the equilibrium temperature is the boiling temperature at ambient pressure.

From equation (1), the droplet heating time is given by:

$$t = \ln\left(\frac{T_{\infty} - T_{do}}{T_{\infty} - T_{dt}}\right) \cdot \frac{M \cdot C_p}{h \cdot A} \quad (2)$$

$T_{do}$  - Droplet temperature at the beginning

$T_{dt}$  - Droplet temperature at the instant  $t$

and the evaporation rate is

$$\frac{dR^2}{dt} = - \frac{2K}{C_p \rho_d} \ln(1+B) \quad (3)$$

Where  $B$  is Spalding mass transfer number defined as  $\frac{C_p (T_{\infty} - T_d)}{h_{fg}}$

For the evaluation of the heat transmission coefficient  $h$  the empirical expression from Ranz and Marshall, which applies a convection correction, was used

$$Nu = \frac{hd}{k} = 2 + 0.6 Re^{1/2} Pr^{2/3} \quad (4)$$

The heat transmission, to the droplet, is a function of the Reynolds number, it increases with the velocity as well as with the droplet diameter, so a drag factor must be evaluated and used to calculate the change of the droplet Reynolds number with time.

### 2.2 Droplet equation of motion

The droplet motion equation is:

$$\frac{d(Mu)}{dt} = - \rho g \frac{u^2}{2} \cdot \pi R^2 \cdot C_d + R_s \quad (5)$$

$R_s$  - source term, includes the gravity forces and others, neglected in this case

$C_d$  - is the drag coefficient, evaluated from the empirical relation proposed by Mellor

$$C_d = 28/Re^{0.85} + 0.48.$$

To determine the relative velocity between the droplet and the gas the initial conditions must be known. The air velocity can be evaluated because the mass flow and the temperature are measured. The droplet velocity at the beginning is not measured, but the atomizer used in the experiments was a twin-fluid atomizer, described in [8], and the initial droplet velocity was assumed to be 15% of the mean stream velocity. As equation (5) shows, the droplet velocity in the control volume is a function of the droplet diameter, so in the measuring volume the droplet concentration is a function of the distance from the injector. Figure 1 shows the droplet volume distributions in a spray evaluated at four different axial stations. In figure 2 the evolution of the relative droplet velocity, for different droplet diameters, can be seen.

### 2.3 Diffracted Pattern

With the equations of motion and heat balance it is possible to evaluate the droplet size distribution in the control volume. Knowing this distribution the evaluation of the diffracted light pattern from a coherent light beam crossing the control volume, is made using the Fraunhofer theory [11]. The light diffracted by the smallest droplets ( $D < 20 \mu m$ ), for which this theory can not be used, is evaluated using the Mie-theory.

### 3. EXPERIMENTAL SET UP AND MEASUREMENTS

Figure 3 shows the experimental set up. In a rectangular channel (20 x 30 mm) an air stream flows at controlled temperature and velocity. In this flow a water film is injected and atomization occurs by the shearing action of the high velocity air stream against the low velocity liquid film. The length of the channel can be changed to allow the measurement of the droplet distribution and concentration at four different downstream distances, 10, 30, 70, 110 mm. The droplet distribution and concentration is measured with an optical method described in [7].

A parallel monochromatic light beam 10 mm diameter from a 5 mW He-Ne laser system, crosses the spray. Some of the light is diffracted due to the droplets, the diffraction pattern depending on the droplet size. A converging lens focuses the non scattered light in the centre of a receiving plane, where a photomultiplier measures the light intensity. Measuring this value with and without spray, enables the evaluation [11] of the liquid volume concentration  $C_v$ , based on the transmission law for polydispersed particles.

$$E/E_0 = \exp(-3/2K C_v \ell/D_{32})$$

$K$  - Mean scattering coefficient

$\ell$  - Spray dimension, crossed by the laser beam (see fig. 3)

Around the focus of the same converging lens a pattern of rings of the diffracted light is formed. Nine concentric circular sectors of photomultipliers measure the diffracted light intensity.

Ten sample-and-hold units were used to guarantee that an instantaneous light profile from the photomultipliers was obtained. The signals were digitized with an A/D converter and the data was stored in paper tape for later processing in a BS 2000 (Siemens) digital computer.

With this system, the diffracted light, which has been shown to be a function of the droplet size distribution, and the transmitted light, which is related to the liquid concentration in the spray, were both measured.

#### 3.2 Measurements

Three sets of measurements have been made, the first one at ambient temperature, one at 200°C and one at 400°C, all at atmospheric pressure.

The influence of the air velocity and water flow rate in the quality of the spray was first studied.

Figure 4 shows that increasing the air velocity, the spray Sauter Mean Diameter decreases, and increasing the water flow rate the Sauter Mean Diameter increases, but only for the smaller air velocities this parameter is important. With air velocity of 120 m/s the change in the water flow from 5 to 20 l/h has no influence in the S.M.D.

These results are in good agreement with the results of Mullinger and Chigier (10).

The air velocity is also important in the liquid volume concentration as figure 5 shows. Increasing the air velocity the liquid volume concentration, measured at the same distance (30 mm) from the injector, decreases. The liquid concentration is proportional to the water flow rate and inversely proportional to the air flow.

Figure 6 shows the influence of the distance in the Sauter Mean Diameter and in the liquid volume concentration for an air velocity of 120 m/s and ambient temperature. The S.M.D. remains constant and the liquid volume concentration decreases. The same can be observed in figures 7 and 8 for two other cases, air velocity 180 and 190 m/s and air temperature 400 and 200 C respectively and water flow rates of 10, 15, 20 l/h. In figure 8 the predicted change in liquid concentration with distance from the injector is also shown (solid lines). The predicted evolution is based on the first measurement of each curve.

The liquid concentration in the control volume changes with axial distance and with the air flow parameters. This is due to the different droplet velocities, the drag force changes with the air velocity and temperature and with the droplet diameter.

As figure 7 shows the droplet diameter does not change with axial distance, no evaporation or coalescence occurs. Predictions of the variation of the droplet diameter with distance from injector, are shown in figure 9, evaluated for case B.

We can see that although case B and C have almost the same velocity the S.M.D. in case C is smaller, this being due to the higher air temperature in case B that causes a worse atomization. For the same reason cases A and B have the same S.M.D. although the air velocities are quite different.

Figure 10 shows the measured and the predicted normalised light profiles for the three different experiments (A, B, C), at 30 mm from the injector.

Table 1  
Experimental conditions

Case	A	B	C
Air vel. (m/s)	120	180	190
Air temp. (°C)	20	400	200
$D_{32}$	45	43	31

Table 1 defines the parameters of experiments A, B, C and the measured Sauter Mean Diameter.

Table 2 contains the measured and predicted values of liquid volume in the control volume.

Table 2  
Liquid volume variation in the control volume (%)  
Water flow rate 10 l/h

dist. (mm)	A	B	C
10	100	100	100
30	81	66(74)	72(72)
70	67	50(47)	53(54)
110	61	42(44)	44(42)

The experimental results, (in brackets) for a water flow of 10 l/h are in good agreement with the theoretical ones.

Case B is where the deviation from predictions is greater (see fig. 8) due to the higher temperature of the air stream that causes a shear layer of two different mediums to interfere with the light beam.

In some cases, interference of the oscillating shear layer between the hot and cold air was noticed.

### 3.3 Source of errors

As figure 10 shows, in the first inner ring the light intensity does not agree with the predictions. This is due to the small radius of the inner ring and the presence of some scattered light even during calibration, made without spray.

We have checked the influence of the oscillating interface between the hot and cold air, and it has been noticed that this influence principally disturbs the first inner ring. It has also been noticed that this influence can be minimised with glass windows in the air channel.

In all the measurements, the first inner ring have not been taken into account.

## 4. CONCLUSIONS

Measurements of the Sauter Mean Diameter of a water spray from a twin-fluid atomizer have been made, for different air temperatures and velocities, using an optical method.

The influence of the air velocity and temperature and of the water flow rate in the spray S.M.D. and in the liquid volume concentration at different distances from the injector have been studied.

The results agree with the predicted ones and with previous measurements made in similar atomizers (10, 12).

Care must be taken when the light beam passes across regions of varying density, as in the case of heated air streams or flames.

## 5. REFERENCES

- [1] - Vicent, M.W., Fuel spray evaporation in gas turbine burners. Ph.d. Thesis, University of Sheffield, 1973.
- [2] - Chidananda, M.S., Eickhoff, H. and Kayser, A., An Analytical Method to Predict Spray Evaporation. DFVLR Internal Report IB 352/79/5.
- [3] - Elkotb, M.M., Fuel Atomization for Spray Modelling, Prog. Energy Combust. Sci. 1982, vol.8, p.61.
- [4] - Law, C.K., Prakash, S. and Sirignano, W.A., Theory of Convective, Transient, Multicomponent Droplet Vaporization, 16th Symposium (Int.) on Combustion, 1976.
- [5] - Yuen, M.C. and Chen, L.W., Heat Transfer Measurements of Evaporating Liquid Droplets. Int. J. Heat and Mass Transfer, vol. 21, p.537, 1978.
- [6] - Felton, P.G., Measurement of Particle Droplet Size Distributions by a Laser Diffraction Technique. Partikel Technologie Nurnberg, Partec 2. 1979, W. Germany.
- [7] - Kayser, A., Zur Optischen Messung der Tropfchengrossenverteilung bei der Zerstaubung von Brennstoff. Chemie Ingenieur Technik 49 (1977), nr. 10 sy 532/77.
- [8] - Kayser, A. and Pita, G., Messungen des Tropfchenspektrums und der Konzentration und Untersuchungen des einfluss der Gemischaufbereitung auf die Schadstoffbildung in der Primarzone einer Gasturbinenbrennkammer. Haus der Technik Vortragsveroeffentlichungen Heft 437 "Verdampfung von Brennstofftropfen und Brennstofffilmen, Vulkan-Verlag, Essen, July 1981.
- [9] - Styles, A.C. and Chigier, N.A., Combustion of Air Blast Atomized spray flames. 16th Symposium (Int.) on Combustion, pag.619, 1976.
- [10] - Mullinger, P.J. and Chigier, N.A., The Design and Performance of Internal Mixing Multijet Twin Fluid Atomizers. J. of Institute of Fuel 251, 1974.

- [11] - Dobbins, R.A., Crocco, L., Glassman, I. Measurement of Mean Particle Sizes of Sprays from Diffractively Scattered Light. AIAA Journal, vol.1, 1963.
- [12] - Wigg, L.D., Drop-Size Prediction for Twin-Fluid Atomizers. - J. Inst. Fuel (1964), 37, 500 - 505.

#### ACKNOWLEDGEMENTS

The author wishes to thank the D.F.V.L.R., Köln, Germany, and specially Prof. G. Winterfeld, Director from the Institut für Antriebs-Technik, for allowing this work to be carried out and presented at this Symposium.

The collaboration received from Dr. Eickhoff and Eng. A. Kayser is acknowledged with pleasure.

AGARD provided the financial support through the Propulsion and Energetics Panel-Program Support to Nations.

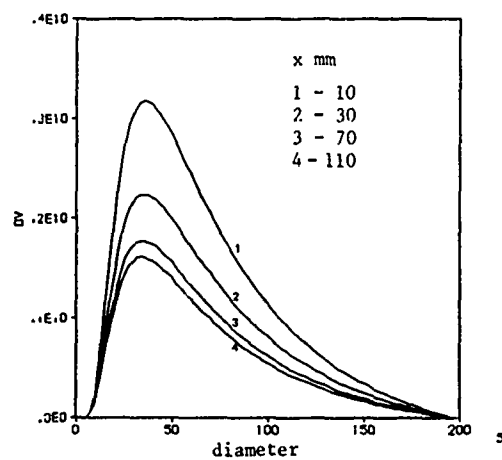


Figure 1. Droplet volume distribution evaluated at four axial stations.

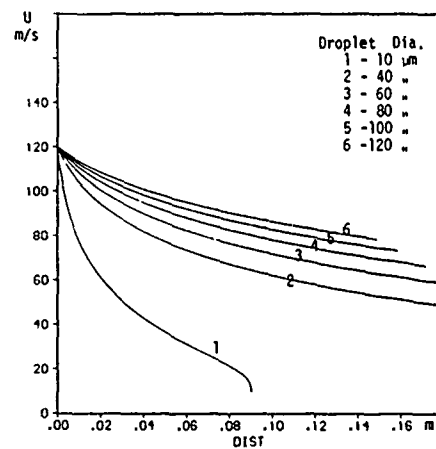


Figure 2. Relative droplet velocity.

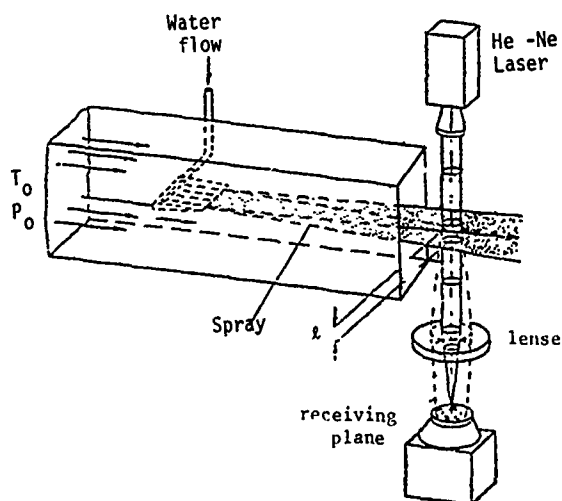


Figure 3. Experimental set up

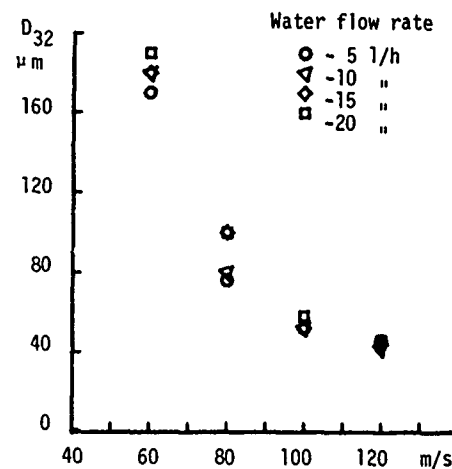


Figure 4. Variation of spray S.M.D. with the air velocity. Axial distance 30 mm.

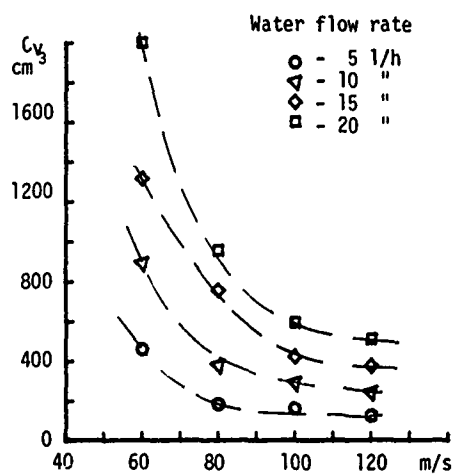


Figure 5. Variation of the liquid volume concentration with the air velocity and with the water flow rate.

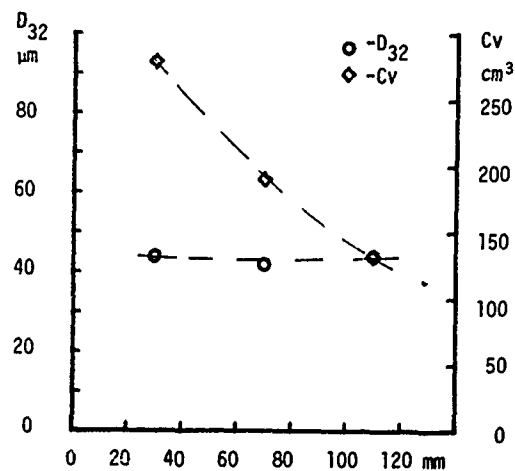


Figure 6. Variation of the S.M.D. and Cv with distance from the injector for case A (air temp. 209°C, air vel. 120 m/s)

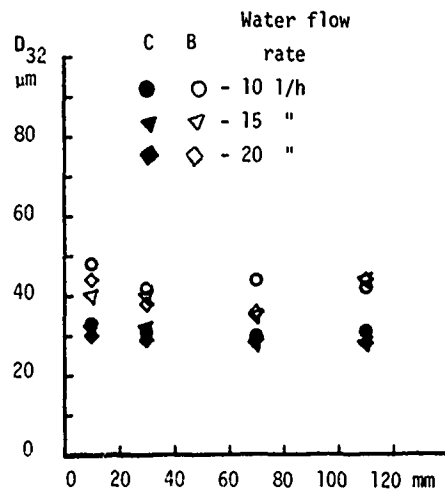


Figure 7. Variation of the S.M.D. with distance from the injector for case B (air temp. 400°C, air vel. 180 m/s) and case C (air temp. 200°C, air vel. 190 m/s)

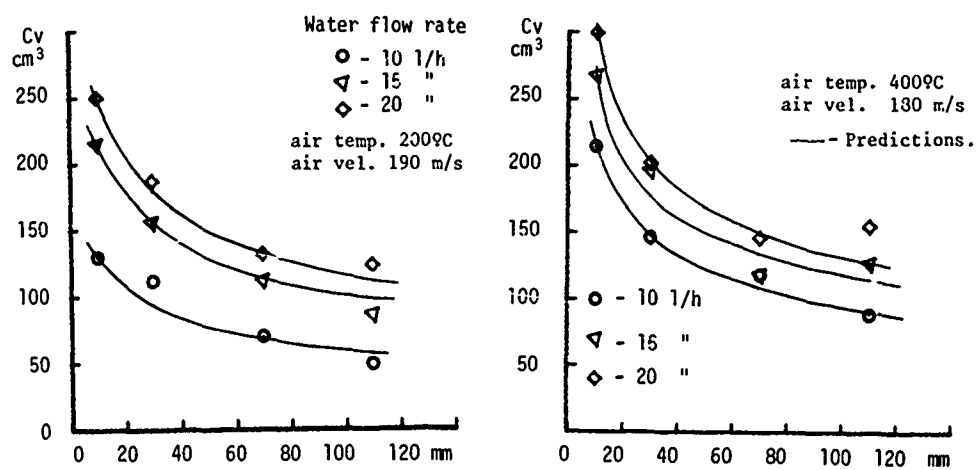


Figure 8. Variation of  $C_v$  with distance from injector, experiments C and B

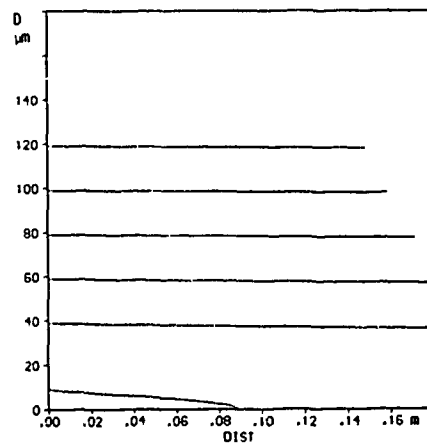


Figure 9. Variation of the droplet diameter with distance (case B).

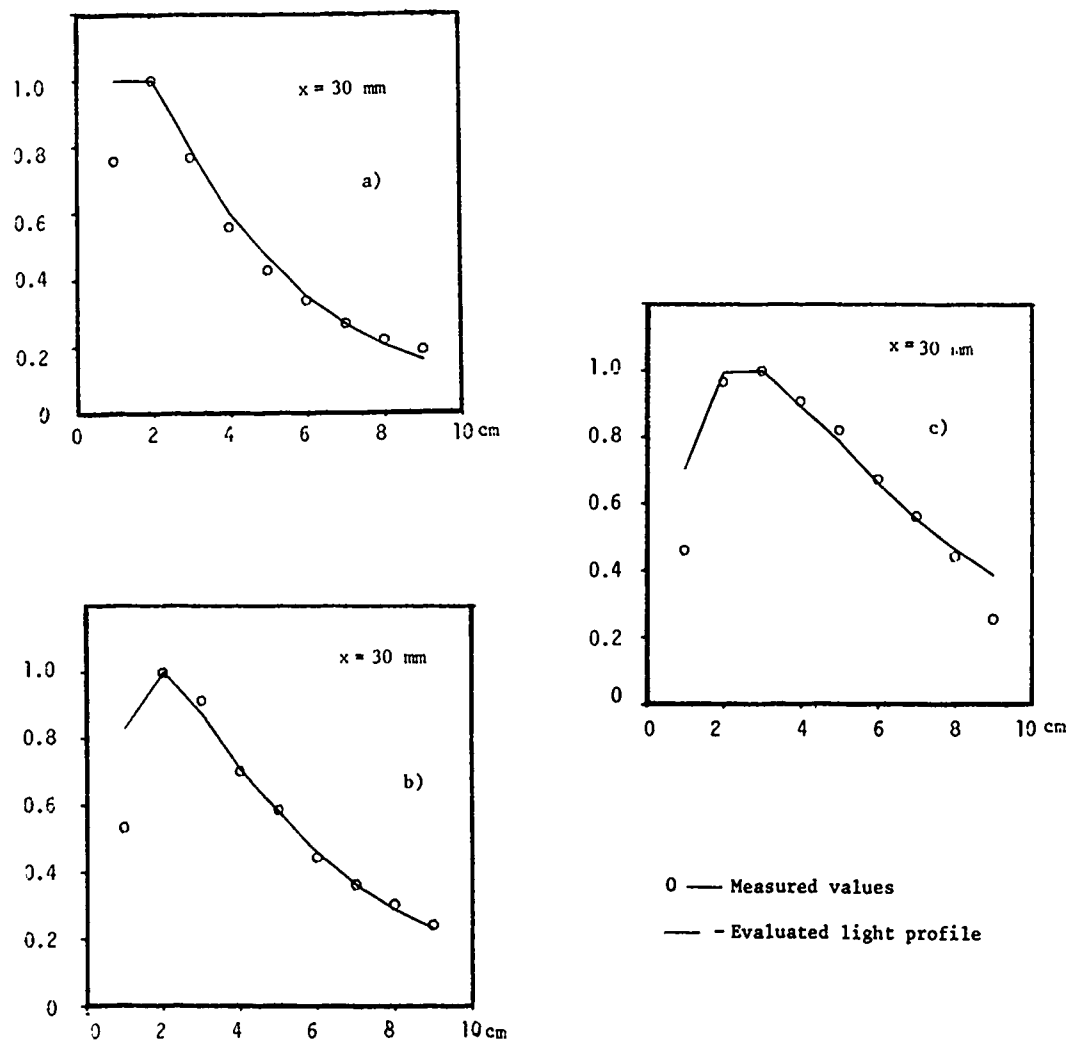


Figure 10. Normalized light profiles



## DISCUSSION

**P.Ramette, Fr**

Vous avez présenté des corrélations en fonction de la vitesse de l'air et du débit du jet. Avez-vous essayé d'exprimer vos résultats en fonction de la vitesse relative du jet par rapport à l'air?

**Réponse d'Auteur**

Non. Nous avons choisi comme variables celles qui correspondent aux mesures directes.

